



Temperature and fuel availability control fire size/severity in the boreal forest of central Northwest Territories, Canada

Dorian M. Gaboriau^{a, b, *}, Cécile C. Remy^c, Martin P. Girardin^{d, e}, Hugo Asselin^{a, d}, Christelle Hély^{b, f, g}, Yves Bergeron^{d, g}, Adam A. Ali^{b, g}

^a School of Indigenous Studies, Université du Québec en Abitibi-Témiscamingue, 445 Boulevard de l'Université, Rouyn-Noranda, QC, J9X 5E4, Canada

^b Institut des Sciences de l'Évolution, UMR 5554 CNRS-IRD-Université Montpellier-EPHE, 2 place Eugène Bataillon, 34095, Montpellier, France

^c Department of Biology, University of New Mexico, Albuquerque, United States

^d Centre for Forest Research, Université du Québec à Montréal, P.O. Box 8888, Stn. Centre-ville, Montréal, QC, H3C 3P8, Canada

^e Natural Resources Canada, Canadian Forest Service, Laurentian Forestry Centre, 1055 rue du PEPS, P.O. Box 10380, Stn. Sainte-Foy, Québec, QC, G1V 4C7, Canada

^f École Pratique des Hautes Études, PSL University, Paris, France

^g Forest Research Institute, Université du Québec en Abitibi-Témiscamingue, 445 Boulevard de l'Université, Rouyn-Noranda, QC, J9X 5E4, Canada

ARTICLE INFO

Article history:

Received 28 July 2020

Received in revised form

26 October 2020

Accepted 1 November 2020

Available online xxx

Keywords:

Large wildfires

Charcoal

Pollen

Fire size

Lake sediments

Vegetation dynamics

Climate change

Holocene

ABSTRACT

The north-central Canadian boreal forest experienced increased occurrence of large and severe wildfires caused by unusually warm temperatures and drought events during the last decade. It is, however, difficult to assess the exceptional nature of this recent wildfire activity, as few long-term records are available in the area. We analyzed macroscopic sedimentary charcoal from four lakes and pollen grains from one of those lakes to reconstruct long-term fire regimes and vegetation histories in the boreal forest of central Northwest Territories. We used regional estimates of past temperature and hydrological changes to identify the climatic drivers of fire activity over the past 10,000 years. Fires were larger and more severe during warm periods (before ca. 5000 cal yrs. BP and during the last 500 years) and when the forest landscape was characterized by high fuel abundance, especially fire-prone spruce. In contrast, colder conditions combined with landscape opening (i.e., lower fuel abundance) during the Neoglacial (after ca. 5000 cal yrs. BP) were related with a decline in fire size and severity. Fire size and severity increased during the last five centuries, but remained within the Holocene range of variability. According to climatic projections, fire size and severity will likely continue to increase in central Northwest Territories in response to warmer conditions, but precipitation variability, combined with increased abundance of deciduous species or opening of the landscape, could limit fire risk in the future.

Crown Copyright © 2020 Published by Elsevier Ltd. All rights reserved.

1. Introduction

The global climate is experiencing rapid warming conducive to increased occurrence of extreme weather events like heatwaves and droughts (IPCC, 2014; Mann et al., 2017). Such conditions may increase the occurrence of exceptionally large and severe wildfires due to the strong positive correlation between temperature and area burned (Abatzoglou and Kolden, 2013; Ali et al., 2012; Duffy

et al., 2005; Gaboriau et al. under review; Kasischke and Turetsky, 2006; Turco et al., 2017). Particularly high temperatures and recurrent droughts during the last decade have led to severe wildfire seasons in forest ecosystems worldwide, for example in Australia (Boer et al., 2020; Nolan et al., 2020), Sweden (SFOR, 2018), Chile (De la Barrera et al., 2018), Greece and the USA (Smith et al., 2019), as well as in the Northwest Territories (NWT) in Canada where about 3.4 million ha burned during the summer of 2014 (Kochubajda et al., 2019; NTENR, 2015).

Large wildfires in the NWT mainly occur from June to September. Lightning-induced fires are predominant and fire frequency and area burned are among the highest in the North American boreal forest (Erni et al., 2020; Veraverbeke et al., 2017). However, the 2014 wildfire season was exceptional in comparison

* Corresponding author. School of Indigenous Studies, Université du Québec en Abitibi-Témiscamingue, 445 Boulevard de l'Université, Rouyn-Noranda, QC, J9X 5E4, Canada.

E-mail addresses: dorian.gaboriau@uqat.ca, gaboriau.dorian@gmail.com (D.M. Gaboriau).

with observations of the last decade (3.4 million ha burned in 2014, compared to a mean of 622 thousand hectares burned annually from 2009 to 2019; Gaboriau et al. under review). More than 380 fires were observed, some of which having burned more than 150,000 ha. Moreover, firefighting costs reached more than CAD 56 million during this exceptional year, compared to an annual mean of CAD 7.5 million in the previous 20 years (NTENR, 2015).

Few remnant trees are left behind in areas burned during large and severe wildfires (Erni et al., 2017; Stephens et al., 2014). Recolonization is dominated by fast-growing pioneer deciduous tree species whose seeds disperse over long distances (Chapin et al., 2010; Walker et al., 2018). Large wildfires also reduce access to ecosystem services (Adams, 2013), cause health issues in human populations (Dodd et al., 2018), and decrease the capacity of Indigenous people to maintain traditional activities on the land (Berkes and Davidson-Hunt, 2006).

Since the 1950s, mean annual temperature increased by over 1.5 °C in Canada, leading to an earlier onset of snowmelt across much of the boreal forest (Zhang et al., 2011). According to climate projections, temperature will continue to rise in the next decades, particularly in the north-central Canadian boreal forest (Price et al., 2013; Wang et al., 2014). Summer and fall precipitation are projected to increase in the boreal forest of Canada and annual precipitation could increase up to 20% by 2100. However, these conditions will not necessarily lead to increased soil and vegetation moisture, as projected warmer temperatures will lead to increased evapotranspiration (IPCC, 2014; Meehl et al., 2007). Hence, the drying effect of higher temperatures in the future will not necessarily be compensated by increased precipitation. Boreal forest landscapes will consequently be altered by a longer growing season (Jain et al., 2018), increased fire activity (Flannigan et al., 2013; Hassol, 2005; Wang et al., 2017; Wotton et al., 2017), higher proportion of deciduous tree species and more open forest canopies than currently (Baltzer et al., submitted; Boulanger et al., 2017;

Chaste et al., 2019; Mekonnen et al., 2019). However, the robustness of the predictions of climate change impacts on wildfire regimes, particularly large wildfires, is limited by our lack of knowledge of the long-term interactions between climate, vegetation and fire (Ali et al., 2012; Conedera et al., 2009; Coogan et al., 2019). While the main drivers of fire activity have been documented in the NWT for the recent past (1965–2016; Gaboriau et al., under review), few palaeoecological data are available at multi-millennial timescales.

To get insights into the long-term relationships between climate, vegetation and fire, we used high-resolution sedimentary proxies (pollen grains and charcoal particles) to reconstruct vegetation and fire histories for the past 10,000 years in the boreal forest of central NWT. We compared the reconstructed vegetation and fire histories with previous studies based on regional climatic reconstructions. Our objectives were (1) to determine whether the recent wildfire regime (last 500 years) is within or outside the Holocene range of variability and (2) to decipher the respective roles of climate and vegetation controls on past fire activity. We expected that the recent fire regime would be characterized by larger and/or more severe wildfires compared to the past 10,000 years in response to ongoing climate warming and recurrent development of severe drought episodes.

2. Material and methods

2.1. Study area and present-day vegetation

We sampled sediments from lakes *Emile*, *Izaak*, *Paradis* and *Saxon* (unofficial names) located north of Yellowknife, in central NWT, and 5–100 km distant from each other (Fig. 1). The sampled lakes have a mean elevation of 382 m (Table 1). According to the Canadian National Fire Database (CNFDB, <http://cwfis.cfs.nrcan.gc.ca/ha/nfdb>), time since the last fire varied between 4 and 39 years in the watersheds of the studied lakes (Table 1). The regional

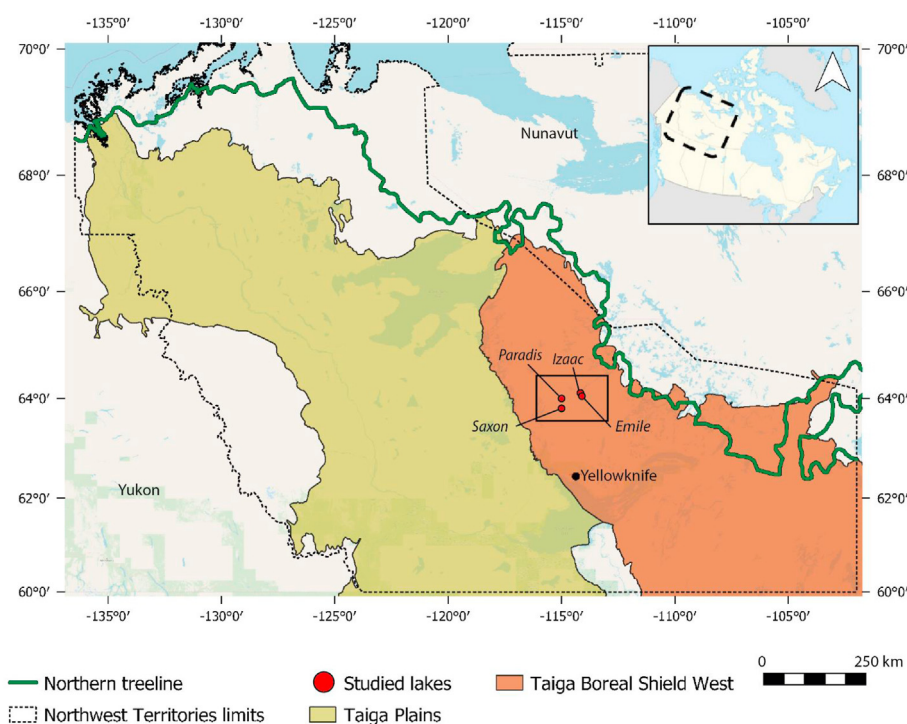


Fig. 1. Locations of the studied lakes in the Northwest Territories (north-central Canada), showing ecozones (adapted from Olson et al., 2001) and treeline (adapted from Timoney et al., 2019).

Table 1

Characteristics of the four studied lakes and sediment records.

Lakes	Emile	Izaac	Paradis	Saxon
Characteristics				
Latitude (°N)	64°03'16.64"	64°05'56.21"	64°00'23.54"	63°48'26.06"
Longitude (°W)	114°06'21.67"	114°10'33.08"	114°59'19.24"	114°58'33.29"
Surface area (ha)	1.4	1.5	1.8	0.9
Elevation (m above sea level)	393	394	347	392
Maximum water depth (cm)	150	115	235	540
Maximum length (m)	203	162	271	177
Lakeshores (Flat/Abrupt)	F	F	F	A
Fluvial input (Present/Absent)	A	A	A	A
Date of the last local fire (CNFD)	2014	2014	1979	1998
Sediment records				
Total length of sediment (cm)	456	359	450	395
Depth of the basal ¹⁴ C date (cm)	448	340	441	350
Sedimentation rate (cm year ⁻¹)	0.049	0.036	0.046	0.036
Median signal-to-noise index	5.4	4.2	4.1	3.7
Total number of significant fire events	57	49	55	46

climate is dry continental, with long cold winters and short warm summers (Environnement Canada, 2017). The study area is located close to the treeline (Timoney et al., 2019) and is part of the Taiga Boreal Shield West ecoregion, characterized by rock outcrops and discontinuous permafrost (Olson et al., 2001). Vegetation is currently dominated by conifer tree species, mostly black spruce (*Picea mariana* (Mill.) B.S.P.). White spruce (*Picea glauca* (Moench) Voss.) is mainly found in the southwestern part of the study area, and jack pine (*Pinus banksiana* Lamb.) mostly occupies the southern part of the NWT, i.e. in the Taiga Plains. Broadleaf tree species are also present in younger stands having regenerated after fire, mostly paper birch (*Betula papyrifera* Marsh) and trembling aspen (*Populus tremuloides* Michx.), such as observed at lake Emile (Appendix S1A). The shrub layer is mainly composed of *Betula glandulosa* Michx., *Alnus alnobetula* (Ehrh.) K. Köch, *Andromeda polifolia* L., *Ledum palustre* L., and *Chamaedaphne calyculata* (L.) Moench. The ground layer is mostly composed of *Vaccinium vitis-idaea* L., *Rubus chamaemorus* L., *Kalmia angustifolia* L. and *Lycopodium annotinum* L., with abundant mosses (mostly *Sphagnum* spp.), while *Cladonia* lichens are found on xeric rock outcrops.

2.2. Past regional climate and vegetation

Previous studies have documented long-term regional climatic and vegetation changes in the northwestern and north-central Canadian boreal forest, which in turn had impacts on wildfire regimes. Before ca. 11,000 cal yrs. BP (calibrated years before present), high solar radiation and summer insolation increased temperatures in the northwestern Canada (Viau et al., 2006), reduced snow cover, and led to the retreat of the Laurentide ice sheet (Dyke, 2005). Deglaciation occurred between ca. 10,000–9000 cal yrs. BP in the study area (Dalton et al., 2020) and left behind numerous lakes and swamps scattered across the landscape (Latifovic et al., 2017; MacDonald, 1995). Following ice retreat, the land was quickly colonized by tundra vegetation soon followed by trees once temperatures warmed during the early Holocene (Dyke, 2005). The Holocene Thermal Maximum (HTM) occurred in northern continental Canada during the mid-Holocene (between 7300 and 4300 cal yrs. BP; Kaufman et al., 2004). During this period, major vegetation reorganization occurred in response to warmer temperature, such as treeline migration to the north and increased abundance of fire-adapted species (i.e. jack pine and black spruce), as observed in the NWT and southwestern Yukon (Gajewski et al., 2014; Pienitz et al., 1999; Sulphur et al., 2016). The decrease in temperature after 4300 cal yrs. BP, characterizing the Neoglacial period, favored coniferous species such as spruce as well as

deciduous shade-tolerant tree species such as paper birch in permafrost-free areas (Moser and MacDonald, 1990; Sulphur et al., 2016). However, interactions between climate, vegetation and fire depend on regional atmospheric and oceanic oscillations, as observed in the eastern Canadian boreal forest where conifer species also increased in density after 3500 cal yrs. BP (Fréchette et al., 2018; Remy et al., 2017).

2.3. Sampling

We sampled lake sediments in June 2018 from the deepest point in each of the four lakes. The vegetation of the watersheds was mainly composed of recently burned conifer tree species and/or shrub birch having grown after the last fire (Appendix S1). The four lakes were small, deep, circular, and characterized by the absence of connections to surrounding watercourses (Table 1). We used a Kajak-Brinkhurst (KB) gravity corer to collect the most recently deposited material at the water-sediment interface (Glew 1991). We subsampled surface sediments on site in 0.5-cm thick sections stocked in plastic bags. We collected deeper sediments in 1-m cores using a 5-cm diameter Russian corer; we wrapped these cores in aluminum foil and placed them in hemicylindrical tubes for protection. We sliced the sediment cores in the laboratory into continuous 1-cm thick subsamples that we stocked in plastic bags and kept refrigerated at 4 °C until analysis. Surface sediments were sampled at a shorter interval (0.5 cm) than deeper sediments (1 cm) to ease comparison with recent (last 500 years) reconstructions of vegetation and fire history.

2.4. Radiocarbon dating and age-depth models

The basal 10 cm of the deepest sediment cores were mostly clay, corresponding to the beginning of lake sedimentation following deglaciation in the four sites, whereas the upper sediment was composed of a gyttja richer in organic matter. We constructed core chronologies based on radiocarbon dating of bulk gyttja samples by ¹⁴C accelerator mass spectrometry (AMS). We used the 'WinBacon' v.2.3.7 R package (Blaauw and Christen, 2011) to reconstruct Bayesian sediment accumulation histories and calibrate age-depth models constructed from seven dates for lakes Emile, Paradis and Saxon and nine dates for lake Izaac (Table S1). We used the IntCal13.14C calibration curve for terrestrial northern hemisphere material (Reimer et al., 2013). We interpolated ages at contiguous 0.5-cm depth intervals and all dates were expressed in calibrated years before present (cal. yrs. BP). We used linear interpolation between ¹⁴C ages rather than best-fit curves, assuming that both

methods yield equivalent chronologies (Blaauw, 2010; Trachsel and Telford, 2017).

2.5. Subsample chemical preparation and charcoal analysis

To distinguish charcoal from other biological material, we applied a common charcoal extraction protocol to each subsample using the 'chemical digestion' method (Winkler, 1985), based on charcoal resistance to chemicals (Mooney and Tinner, 2011). We removed a 1.4-cm³ subsample from each liquid subsample of surface sediment (KB) and 1-cm³ for the rest of the core (solid part), following Mustaphi et al. (2015). We took sediments in the central part of each core slice to limit the risk of contamination with modern material. We deflocculated and bleached the subsamples by placing them in a potassium hydroxide (KOH) solution combined with bleach and sodium hexametaphosphate – (NaPO₃)₆ – on a stirring table for 24 h at room temperature; which later allowed us to differentiate black charcoal from bleached organic matter (Braadbaart and Poole, 2008; Swain, 1973). We wet-sieved the solution through a 160 µm mesh to collect larger charcoal particles produced by fire events having mostly occurred 0–3 km from the lakeshore (Oris et al., 2014). We sorted charcoal particles in a Petri dish, and measured their area using a camera (D-Moticam 1080, Motic Images, 2018) mounted on a binocular microscope and connected to an image-analysis software (MOTICAM IMAGE Plus 3.0).

2.6. Fire history reconstruction

We reconstructed burned biomass (hereafter *BB*; unitless) at each study site by measuring the cumulative area of charcoal particles per cm³ for each subsample. Based on numerical age-depth models, we transformed this measure into charcoal accumulation rate (hereafter *CHAR*, i.e. mm² cm⁻² yr⁻¹), using the R package 'paleofire' v.1.2.3 (Blarquez et al., 2014). We pooled and smoothed these series (using a 500-year window) by (1) rescaling initial *CHAR* values using min-max transformation, (2) homogenizing the variance using Box-Cox transformation, and (3) rescaling the values to Z-scores (Power et al., 2008). The resulting values (cumulative charcoal area) are interpreted as representing the regional signature of fires having occurred in the watersheds of the studied lakes, and thus the regional burned biomass (hereafter *RegBB*; unitless).

We detected past fire events (Appendix S2) within each individual *CHAR* series using the CharAnalysis v.1.1 software (Higuera, 2009; available at <https://github.com/phiguera/CharAnalysis>). Following Brossier et al. (2014), we used the narrowest time window allowing us to obtain a median Signal-to-Noise Index greater than 3.0 (Table 1). We obtained the past regional fire frequency (hereafter *RegFF*; fire.year⁻¹) by combining the smoothed series using the R package 'paleofire' v.1.2.3 (Blarquez et al., 2014). We assessed the significance of changes in *RegFF* and *RegBB* by using a bootstrap procedure with 999 iterations (BCI; 90%).

Following Ali et al. (2012), we added a constant equal to 1 to *RegBB* and *RegFF* and we computed the ratio (*FS* index), which we interpreted as indicating fire size and/or severity. The *FS* index corresponds to mean burned biomass per fire calculated for 500-year intervals, and thus, reflects fire size. Considering that large fires in boreal North America are known to cause high vegetation mortality, the *FS* index could also represent fire severity (Ali et al., 2012; Cansler and McKenzie, 2014; Hély et al., 2020; Hennebelle et al., 2020; Kelly et al., 2013). We assumed that high *FS* index values corresponded to periods when the study area experienced larger and more severe wildfires. Following Power et al. (2008), we used a reference period, here corresponding to 500–0 cal yrs. BP (by

convention, 0 cal. yr. BP corresponding to AD 1950), to calculate *RegBB*, *RegFF* and *FS* index anomalies.

2.7. Vegetation history reconstruction

We reconstructed the Holocene vegetation history using palynological analysis of subsamples of bulk sediment (1 cm³) taken at regular 4 cm intervals along the core of lake *Emile*. We counted and determined pollen and spores in sediment subsamples using standard techniques described by Faegri and Iversen (1989). We counted a minimum of 300 pollen grains of terrestrial taxa for each subsample (Djamali and Cillerio, 2020), under a microscope with a × 200 or × 400 magnification factor. We identified pollen grains based on the Pollen Atlas of Arctic and Boreal Canada (Williams, 2006) and pollen keys from (Vincent, 1973) and Richard (1970). We identified tree pollen to the genus level. We also identified the green algae *Pediastrum* and spores of aquatic plants. We added exotic marker pollen (*Eucalyptus*) to each subsample to estimate pollen concentration (grains cm³) and pollen accumulation rate (*n* grains cm⁻² yr⁻¹) for taxa with an average percentage greater than 0.1% (Appendix S3), using the R package 'rioja' (Juggins, 2017). We measured the total pollen accumulation rate (PAR), based on all terrestrial taxa with percentages greater than 0.1%.

2.8. Temperature and drought

We used quantitative temperature reconstructions from four different proxies (described in Appendix S4) and originating from northwestern and north-central Canada (Lecavalier et al., 2017; Porter et al., 2019; Upiter et al., 2014; Viau et al., 2006). The reconstructions included (i) mean air temperature in July from 6000 cal yrs. BP to present estimated from chironomid assemblages sampled in lake sediments of the central Northwest Territories (Upiter et al., 2014), (ii) mean summer temperature anomalies relative to the 1961–1990 period in central Yukon, from 10,000 cal yrs. BP to present, estimated using precipitation isotopes in syngenetic permafrost (Porter et al., 2019), (iii) mean Arctic summer air temperature anomalies relative to the preindustrial period reconstructed from ice melt in the Agassiz ice cap (Ellesmere Island, Northwest Territories) (Lecavalier et al., 2017), and (iv) mean July temperature estimated from pollen records for the past 10,000 years across northwestern North America (Viau et al., 2006). We assumed that these reconstructions captured temperature fluctuations during the summer months, i.e. the period of warm and dry weather conducive to wildfire activity in the boreal forest. For each reconstruction, we interpolated and standardized values for each year between 10,000 cal yrs. BP and present, converting the data in anomalies relative to the mean for the entire period. We then averaged the four reconstructions. Then, we assessed the significance of temporal changes in temperature by bootstrapping the pooled means 999 times (BCI; 90%). We present temperature anomalies relative to the reference period 500–0 cal yrs. BP.

To quantify the relationships among the fire, vegetation and temperature time series reconstructed at different temporal resolutions, and to avoid interpolation when time series were not sampled at identical points, we measured the Pearson correlation coefficient with 95% confidence interval between the automatically binned undetrended time series following Mudelsee (2013) and using the R package 'BINCOR' (Polanco-Martinez et al., 2019).

We used three indicators of hydrological variability to define Holocene dryness periods assumed to correspond to low vegetation productivity (inferred from pollen and plant macrofossil assemblages) and low lake water levels (inferred from diatoms) (Lauriol et al., 2009; Pienitz et al., 1999; Viau and Gajewski, 2009). We compared these records providing independent evidence of

dryness periods with our fire reconstructions to detect possible temporal overlap of specific fire regimes and dryness periods.

3. Results

3.1. Age-depth models

Core length varied from 359 cm at lake *Izaak* to 456 cm at lake *Emile* (Table S1). According to the Bayesian age-depth models, basal sediments were dated between ca. 10,000 cal yrs. BP at lake *Saxon* and ca. 9530 cal yrs. BP at lake *Izaak* (Fig. 2). We used 9530 cal yrs. BP as the earliest date for wildfire regime reconstructions, as it was included in all four reconstructions. The four age-depth models had similar sedimentation rates, varying between 0.036 cm and 0.049 cm year⁻¹ (Table 1), similar to the results a previous study of other boreal lakes in the NWT (Crann et al., 2015).

3.2. Regional fire history

The regional fire activity remained fairly constant throughout the Holocene with approximately 5 fires per millennium (+2 anomaly; Fig. 3A). Mean *RegFF* very slightly increased from ca. 9500 cal yrs. BP to ca. 500 cal yrs. BP, before decreasing during the reference period (500–0 cal. BP). *RegBB* steadily increased starting from ca. 9500 cal yrs. BP, peaked between ca. 7000–5000 cal yrs. BP, before gradually decreasing to present values, the lowest of the entire series (Fig. 3B). Higher *FS* index values were recorded before 4000 cal yrs. BP (Fig. 3C), and, although to a lesser extent, during the reference period (500–0 cal yrs. BP).

3.3. Vegetation history

We identified a total of 41 pollen taxa in the whole sequence extracted at lake *Emile*, covering the period from ca. 9700 cal yrs. BP to present. Eighteen taxa had a mean pollen percentage >0.1% over the entire study period (Appendix S3). The PAR diagram is dominated by few tree and shrub taxa throughout the sequence (*Picea*, *Betula*, *Pinus* and *Alnus*; Fig. 4). *Artemisia*, Cyperaceae, Ericaceae, Poaceae, *Juniperus*, *Larix* and *Salix* were also present, but in low numbers.

PAR was low from ca. 9700 to 7800 cal yrs. BP, concomitant with a stable and relatively low sedimentation rate (Fig. 4). Most trees and shrubs were relatively low, except *Populus*, *Myrica* and *Lycopodium*, which recorded their highest values at that time. A marked increase of *Picea* (likely black spruce, MacDonald et al., 1993) occurred ca. 7800 cal yrs. BP, along with a simultaneous expansion of *Alnus alnobetula* subsp. *crispa*. At the same time, the lake recorded a major decrease in *Populus*, *Myrica* and *Lycopodium*. PAR increased markedly, while the sedimentation rate remained stable. PAR, *Picea* and *Alnus alnobetula* subsp. *crispa* remained high until ca. 6000 cal yrs. BP, before decreasing, concomitant with an increase of the sedimentation rate ca. 5700 cal yrs. BP. *Pinus* (likely jack pine; Sulphur et al., 2016), *Betula* and *Alnus incana* subsp. *rugosa* increased somewhat later, while the sedimentation rate remained high. After ca. 4000 cal yrs. BP, the sedimentation rate decreased and remained stable for the last two millennia of the record, while *Pinus* remained relatively high, especially after ca. 2500 cal yrs. BP. A short-duration PAR peak occurred between ca. 3000 and 2200 cal yrs. BP, although the sedimentation rate remained stable.

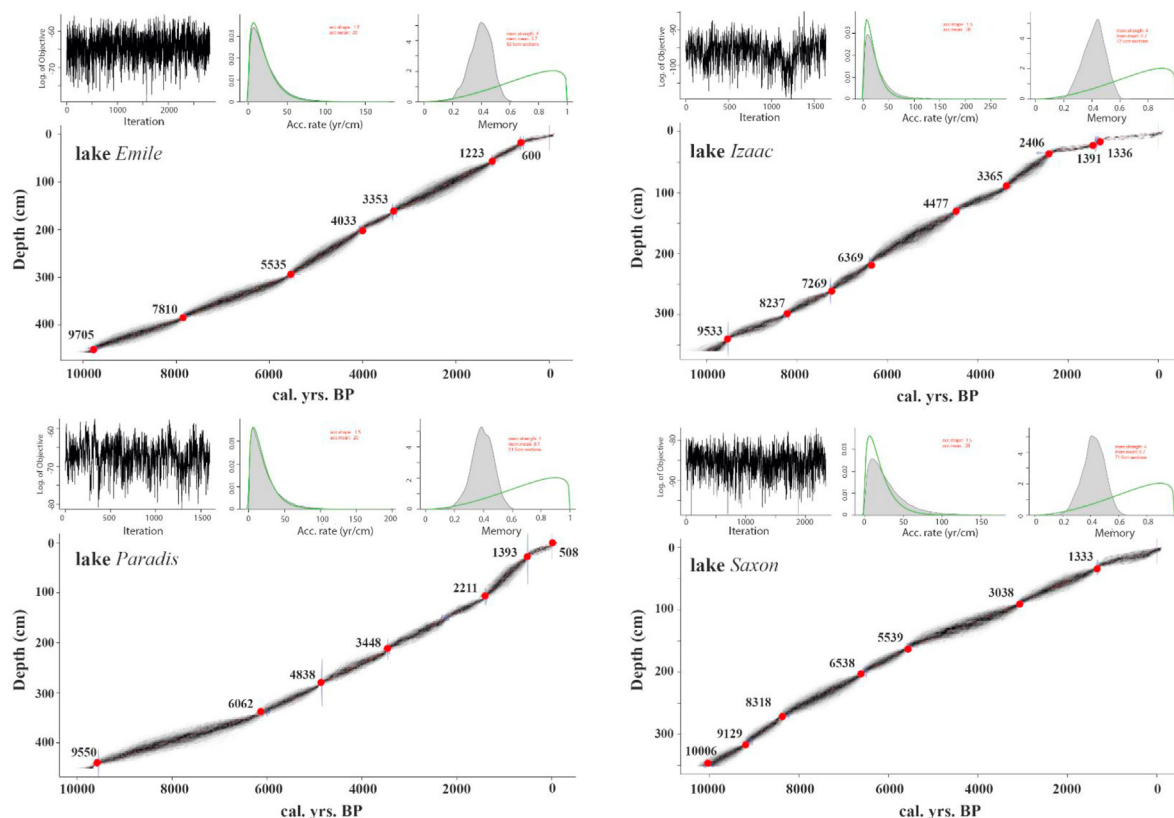


Fig. 2. WinBacon outputs for lakes *Emile*, *Izaak*, *Paradis* and *Saxon*. Upper left panels describe the MCMC (Markov Chain Monte Carlo) iterations (the distribution is stationary with little structure among neighbouring iterations). Upper middle panels show the distribution of sediment accumulation rates. Upper right panels show the memory corresponding to the variation of sediment accumulation rate in time. Main panels show the calibrated ¹⁴C dates (see Table S1 for full details on the chronology) and age-depth models (with 95% confidence intervals).

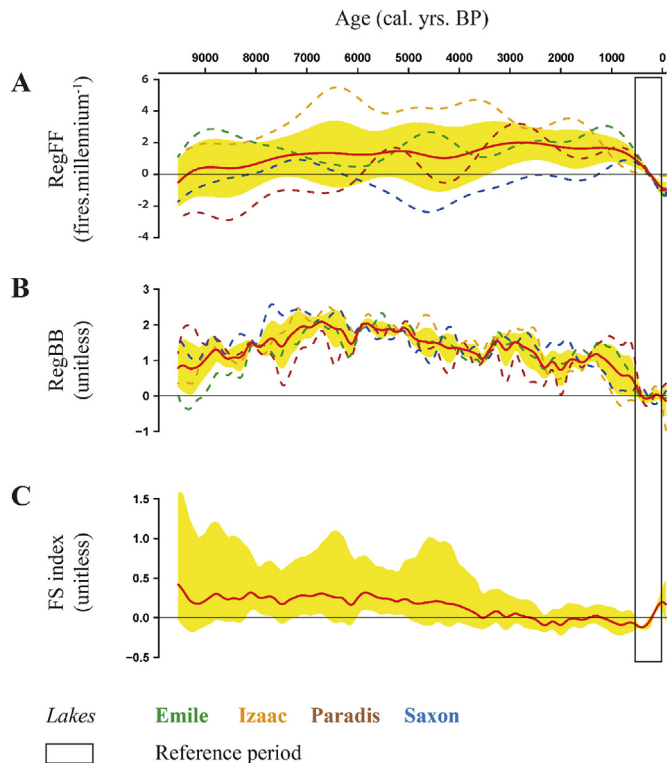


Fig. 3. Holocene fire activity anomalies interpolated using a 500-year bandwidth smoothing, relative to the 500–0 cal yrs. BP reference period (black horizontal line) for individual and regional fire-history reconstructions based on sediment charcoal records from lakes Emile, Isaac, Paradis and Saxon: (A) Regional Fire Frequency (RegFF), (B) Regional Biomass Burning (RegBB) and (C) Fire Size/Severity (FS index) based on regional biomass burning and fire frequency. Yellow shaded areas in each panel represent the 90% bootstrap confidence intervals. (For interpretation of the references to colour in this figure legend, the reader is referred to the Web version of this article.)

Pediastrum and *Nuphar* increased simultaneously ca. 2200 cal yrs. BP. During the last two millennia, *Picea*, *Pinus*, *Betula* and *Alnus* sp. decreased, while *Ericaceae* and *Cyperaceae* remained stable or even slightly increased, such as for *Juniperus*. The sedimentation rate decreased after 500 cal yrs. BP, following a slight increase between ca. 1500 and 500 cal yrs. BP.

3.4. Temperature and drought

We identified three main climatic periods over the Holocene, based on pooled summer temperature reconstructions (Fig. 5). Larger confidence intervals reveal more uncertainty in temperature estimations from 10,000 to 6500 cal yrs. BP, corresponding to the early Holocene period. Overall, maximum temperature values were recorded between ca. 6500 and 4500 cal yrs. BP, before decreasing until ca. 1500 cal yrs. BP, and increasing again drastically during the last few centuries. According to inferred hydrological conditions (Fig. 6; Lauriol et al., 2009; Pienitz et al., 1999; Viau and Gajewski, 2009), the period between ca. 7000–3000 cal yrs. BP was characterized by wetter conditions in central NWT and northern Yukon, compared to the rest of the study period. A major change in diatom-inferred dissolved organic carbon at ca. 5800 cal yrs. BP suggests a warm and humid interval during the mid-Holocene (Fig. 6a; Pienitz et al., 1999), resulting in high lake productivity (Fig. 6c; Lauriol et al., 2009). Conversely, high annual precipitation were recorded before ca. 7500 cal yrs. BP and around ca. 1000 cal yrs. BP (Fig. 6b; Viau and Gajewski, 2009).

3.5. Relationships between fire, temperature and vegetation

Warm periods (ca. 10,000 to 5000 cal yrs. BP and last 500 years) coincided with low RegFF, high FS index, and relatively high RegBB (Table 2). Higher temperatures corresponded with higher *Populus*, *Myrica* and *Lycopodium* abundance. A cooler period (ca. 5000–500 cal yrs. BP) was characterized by a low FS index and a landscape richer in *Pinus*, *Larix*, *Juniperus*, *Poaceae*, *Pediastrum* and *Nuphar* (Table 2). PAR, interpreted as fuel availability, coincided with high RegFF and high RegBB, especially for *Picea*, *Betula* and *Alnus alnobetula* subsp. *crispa* (Table 2).

4. Discussion

Our fire history reconstructions based on macroscopic sedimentary charcoal provide evidence that fire size and/or severity were higher during warmer periods (i.e. before ca. 5000 cal yrs. BP and during the last 500 years) than during the Neoglacial (after ca. 5000 cal yrs. BP). During the Holocene, the RegBB metric was positively correlated with the FS index because RegFF was relatively constant from the early to the late Holocene.

4.1. Fire, climate and vegetation interactions

4.1.1. Early Holocene (10,000–6500 cal yrs. BP)

The spatial variability of the climate data used in air temperature reconstructions shown by the large confidence interval around summer temperature during the early Holocene (i.e. before 6500 cal yrs. BP; Fig. 5) is due to differences in time of deglaciation across northern Canada (Dyke, 2005; Kaufman et al., 2004). Summers were warmer in far northern NWT and in central Yukon (Lecavalier et al., 2017; Porter et al., 2019) but cooler in north-western Canada (Viau et al., 2006), probably due to a later time of deglaciation. Conditions were also dry at this time in north-central Canada but not in northwestern Canada (i.e. Mackenzie region; Fig. 6), confirming the presence of the Laurentide ice sheet in the study area during the early Holocene. PAR indicates that the first stage of vegetation colonization following ice retreat was characterized by an open woodland, as observed in previous studies for the same period and in the same area (Conedera et al., 2009; Macumber et al., 2011; Sulphur et al., 2016). The landscape was dominated by pioneer taxa such as *Populus* and *Betula* (likely dwarf birch, Andrews et al., 1980). The relatively high percentages of *Picea* spp. (~40–50%) was likely due to long-distance transport of pollen by wind, from populations located to the southwest of the study area (Campbell et al., 1999). Low tree abundance before 8000 cal yrs. BP can be explained by the time required for northward migration following deglaciation (Gajewski et al., 1993; Moser and MacDonald, 1990; Ritchie, 1985). Dry conditions also could have limited tree cover. During the early Holocene, deciduous shrubs, less inflammable than conifer trees, and low fuel abundance likely limited fire ignition and spread, but might have promoted large and/or severe fires in shrub areas during dry years.

4.1.2. Mid-Holocene (6500–5000 cal yrs. BP)

Warmer and wetter climate during the mid-Holocene in northern continental Canada (Kaufman et al., 2004; Porter et al., 2019; Ritchie et al., 1983) favored tree growth, leading to gradual densification of the vegetation cover as suggested by the increase in PAR values despite a relatively stable sedimentation rate. This result is in line with previous reconstructions in southwestern Yukon (Cwynar and Spear, 1995; Gajewski et al., 2014), Alaska (Tinner et al., 2006) and Northwest Territories (Sulphur et al., 2016). Warm temperature and wet conditions of the mid-Holocene especially favored dense conifer forests (*Picea* and *Pinus* spp.),

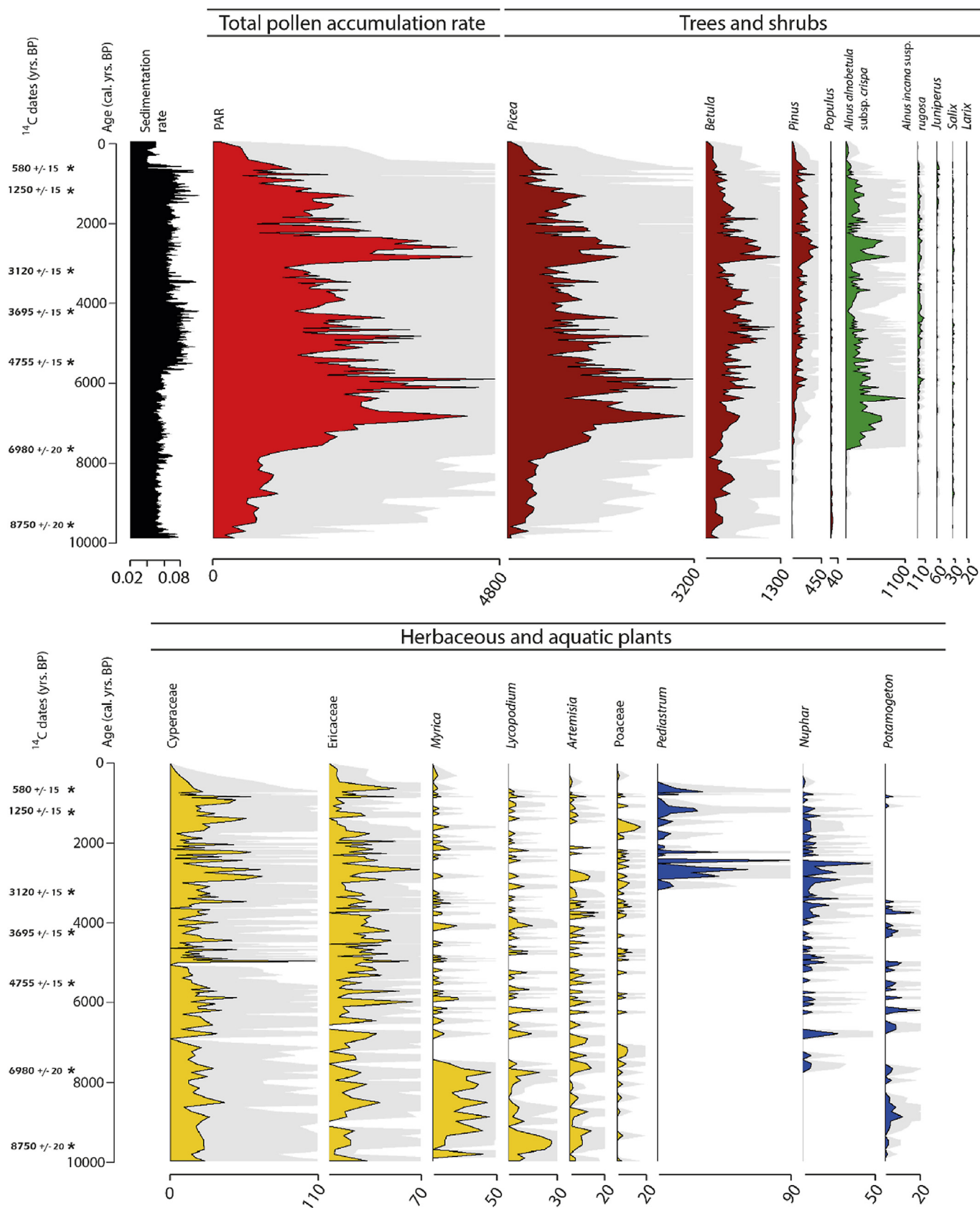


Fig. 4. Sedimentation ($\text{cm}^{-1} \text{year}^{-1}$) and pollen accumulation rates ($\text{grains cm}^{-2} \text{year}^{-1}$) at lake Emile for total terrestrial pollen (PAR, in red) and for the main taxa: trees (in brown), shrubs (in green), herbaceous plants (in yellow) and green algae (*Coenobium*) and aquatic plants (in blue) all having an average percentage greater than 0.1% over the entire study period. Pale areas represent $\times 5$ rescaling. Note that the scale differs for each pollen or spore taxon. (For interpretation of the references to colour in this figure legend, the reader is referred to the Web version of this article.)

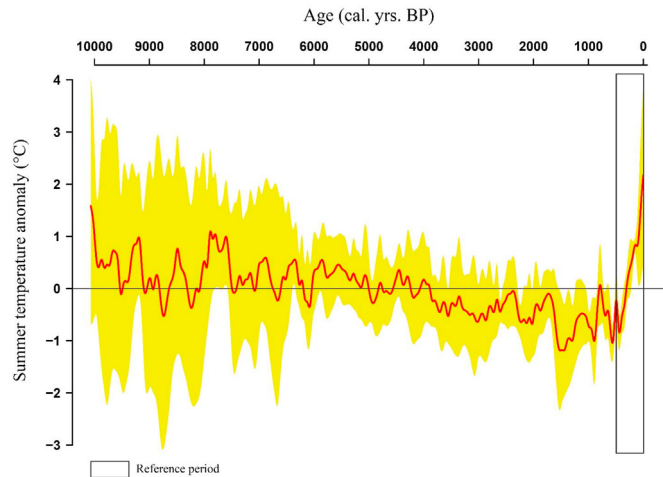


Fig. 5. Mean summer temperature anomalies over the Holocene, relative to the 500–0 cal yrs. BP reference period, obtained from the calculation of the means of standardized independent temperature datasets described in Appendix S4. The yellow shaded area indicates the 90% bootstrap confidence interval. (For interpretation of the references to colour in this figure legend, the reader is referred to the Web version of this article.)

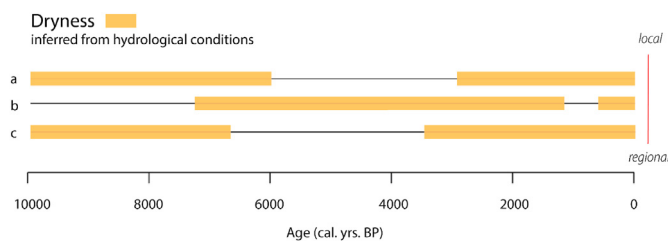


Fig. 6. Dryness periods inferred from hydrological conditions from different locations in north-central and northwestern Canada. Distance from the study area increases from top to bottom. (a) Central Northwest Territories (Pienitz et al., 1999; dissolved organic carbon (DOC) inferred from diatom assemblages). (b) Mackenzie region (50°–70°N, 120°–140°W; Viau and Gajewski, 2009; annual precipitation inferred from pollen assemblages). (c) Northern Yukon (Lauriol et al., 2009; lake-level inferred from plant macrofossil analysis).

Table 2

BINCOR Pearson correlation coefficient (with 95% confidence interval) between fire metrics, temperature, total pollen accumulation rate (PAR), and accumulation rates of taxa with an average percentage greater than 0.1% over the entire study period. *** $p < 0.001$, ** $p < 0.01$ and * $p < 0.05$.

	RegFF	RegBB	FS index	Temperature
Temperature	–0.53 [–0.63, –0.42]***	0.21 [0.07, 0.35]**	0.66 [0.58, 0.74]***	–
PAR	0.50 [0.35, 0.62]***	0.58 [0.45, 0.68]***	0.14 [–0.04, 0.31]	–0.13 [–0.30, 0.04]
Picea	0.37 [0.21, 0.51]***	0.64 [0.53, 0.74]***	0.29 [0.12, 0.44]**	0.00 [–0.17, 0.17]
Pinus	0.63 [0.52, 0.72]***	–0.16 [–0.32, 0.00]	–0.56 [–0.67, –0.44]***	–0.52 [–0.63, –0.39]***
Betula	0.27 [0.12, 0.42]***	0.31 [0.16, 0.45]***	0.09 [–0.08, 0.25]	–0.06 [–0.22, 0.1]
Populus	–0.34 [–0.47, –0.18]***	0.04 [–0.13, 0.20]	0.28 [0.12, 0.43]***	0.18 [0.02, 0.34]*
Alnus alnobetula subsp. crispa	0.40 [0.25, 0.53]***	0.42 [0.28, 0.55]***	0.09 [–0.08, 0.25]	–0.02 [–0.18, 0.14]
Alnus incana subsp. rugosa	0.23 [0.07, 0.38]**	0.16 [0.00, 0.32]*	–0.02 [–0.18, 0.15]	–0.14 [–0.30, 0.02]
Juniperus	0.09 [–0.08, 0.25]	–0.30 [–0.45, –0.15]***	–0.33 [–0.47, –0.17]***	–0.38 [–0.51, –0.23]***
Salix	0.21 [0.05, 0.36]*	0.10 [–0.06, 0.26]	–0.04 [–0.21, 0.12]	–0.17 [–0.32, –0.01]*
Larix	0.21 [0.05, 0.36]*	–0.23 [–0.38, –0.07]**	–0.34 [–0.48, –0.19]***	–0.26 [–0.41, –0.1]**
Cyperaceae	0.20 [0.03, 0.35]*	–0.01 [–0.17, 0.15]	–0.13 [–0.29, 0.03]	–0.19 [–0.34, –0.03]*
Ericaceae	0.14 [–0.03, 0.29]	0.11 [–0.06, 0.27]	0.00 [–0.16, 0.17]	0.01 [–0.15, 0.17]
Artemisia	–0.05 [–0.22, 0.11]	0.10 [–0.06, 0.26]	0.13 [–0.04, 0.29]	0.15 [–0.01, 0.31]
Myrica	–0.46 [–0.58, –0.32]***	–0.01 [–0.17, 0.16]	0.33 [0.17, 0.47]***	0.38 [0.23, 0.51]***
Lycopodium	–0.31 [–0.45, –0.15]***	–0.05 [–0.21, 0.12]	0.19 [0.03, 0.35]*	0.2 [0.04, 0.35]*
Poaceae	0.23 [0.07, 0.38]**	–0.04 [–0.21, 0.12]	–0.19 [–0.34, –0.02]*	–0.24 [–0.39, –0.08]**
Pediastrum	0.28 [0.12, 0.43]***	–0.23 [–0.38, –0.07]**	–0.37 [–0.5, –0.22]***	–0.23 [–0.38, –0.07]**
Potamogeton	–0.14 [–0.30, 0.02]	0.14 [–0.02, 0.30]	0.22 [0.06, 0.37]**	0.10 [–0.06, 0.26]
Nuphar	0.38 [0.23, 0.51]***	0.01 [–0.15, 0.18]	–0.24 [–0.39, –0.08]**	–0.24 [–0.39, –0.08]**

causing fuel accumulation conducive to large and severe fires, as previously observed in Alaska (Hoecker et al., 2020). During this period, wet conditions limited the increase in fire frequency (RegFF), which remained stable, while biomass burning (RegBB) was higher. Because the period was wet, it suggests that these non-frequent large wildfires occurred during episodic drought that dried the fuel and favored fire spread. High fire activity during the mid-Holocene promoted fire-prone coniferous species (*Picea* and *Pinus*) and pioneer trees and shrubs (*Betula* and *Alnus*), as previously observed in the study area (Parisien et al., 2020).

4.1.3. Neoglacial (5000–1000 cal yrs. BP)

The Neoglacial was characterized by a gradual decrease in temperature, reaching an all-time low ca. 1500 cal yrs. BP. Cooling favored the expansion of *Pediastrum* and *Nuphar* ca. 3000 cal yrs. BP, as observed in Alaska (Edwards et al., 2000). The Neoglacial was also characterized by landscape opening, as shown by a decrease in *Picea* and increase in *Poaceae*, also observed in previous studies (MacDonald, 1995; Pienitz et al., 1999). Lower fuel abundance, likely due to cooler and drier conditions less favorable to shrub and tree productivity, hindered fire spread leading to lower biomass burned.

4.1.4. Last millennium (1000–0 cal yrs. BP)

During the last 1000 years, temperature varied but remained low until ca. 500 cal yrs. BP before a marked increase, especially during the last century. Vegetation density and fire frequency were as low as during the early Holocene, while RegBB reached its lowest levels for the entire time series. Contrary to our expectations, the recent fire size/severity (i.e. over the last 500 years) is below the maximum values observed during the mid-Holocene.

4.2. Implications for future fire risk

We provide evidence that both climate conditions and vegetation dynamics played a key role in shaping the wildfire regime over the past 10,000 years in central NWT. Fire size and/or severity were higher under the warmer and wetter climate of the mid-Holocene (7000 to 5000 cal yrs. BP), which favored fuel availability, corroborating recent observations on large wildfires during the last decades in the study area (Gaboriau et al. under review). Our results can be used to anticipate future fire risk and to elaborate risk mitigation strategies including fuel management.

While temperature is expected to continue increasing in western Canada over the 21st century, dryness periods could be more severe than in the past (Price et al., 2013). Hence, fire frequency might increase (Wotton et al., 2017), but not necessarily biomass burning. Indeed, temperature increase could lead to the conversion of coniferous to deciduous forests (Hansen et al., in press; Mekonnen et al., 2019), or to a more open landscape (Asselin and Payette, 2005; Baltzer et al., submitted), which would negatively feedback on fire ignition and spread by reducing fuel flammability, combustibility, and/or connectivity. Hence, for large wildfires to be frequent in the future, the warming-induced increase in evapotranspiration will have to be compensated by increased precipitation to produce sufficient fuel (Flannigan et al., 2016).

Author contributions

Dorian M. Gaboriau: Conceptualization, Methodology, Formal analysis, Writing - original draft, Writing - review & editing Cécile C. Remy: Methodology, Software, Writing - review & editing Martin P. Girardin: Conceptualization, Investigation, Hugo Asselin: Conceptualization, Methodology, Investigation, Supervision, Validation, Writing - review & editing Christelle Hély: Writing - review & editing, Yves Bergeron: Funding acquisition, Writing - review & editing, Adam A. Ali: Conceptualization, Methodology, Supervision, Project administration, Investigation, Validation, Writing - review & editing.

Declaration of competing interest

The authors declare that they have no known competing financial interests or personal relationships that could have appeared to influence the work reported in this paper.

Acknowledgements

We thank Benoît Brossier, David Gervais, Julia Morarin, Laure Paradis and David Pretorius for their assistance in the field. We are also grateful to Christine Simard for her help in identifying charcoal fragments, Jordan Paillard for pollen counting and identification and Pierre J. H. Richard for suggestions on an earlier draft. This work was supported by Polar Knowledge Canada (Grant # NST-1718-0014), the Natural Sciences and Engineering Research Council of Canada, the Canadian Forest Service, the National Geography Society (Grant # EC-386R-18), and the French University Institute (IUF).

Data and R codes used in this manuscript are available on <https://github.com/dgaboriau/Research-data>. Pollen and fire datasets are respectively available on www.neotomadb.org and www.paleofire.org.

Appendix A. Supplementary data

Supplementary data to this article can be found online at <https://doi.org/10.1016/j.quascirev.2020.106697>.

References

Abatzoglou, J.T., Kolden, C.A., 2013. Relationships between climate and macroscale area burned in the western United States. *Int. J. Wildland Fire* 22, 1003–1020.

Adams, M.A., 2013. Mega-fires, tipping points and ecosystem services: managing forests and woodlands in an uncertain future. *For. Ecol. Manag.* 294, 250–261.

Ali, A.A., Blarquez, O., Girardin, M.P., Hély, C., Tinquaut, F., El Guellab, A., Valsecchi, V., Terrier, A., Bremond, L., Genies, A., 2012. Control of the multi-millennial wildfire size in boreal North America by spring climatic conditions. *Proc. Natl. Acad. Sci. Unit. States Am.* 109, 20966–20970.

Andrews, J.T., Mode, W.N., Webber, P.J., Miller, G.H., Jacobs, J.D., 1980. Report on the distribution of dwarf birches and present pollen rain, Baffin Island, NWT,

Canada. *Arctic* 33, 50–58.

Asselin, H., Payette, S., 2005. Late Holocene opening of the forest tundra landscape in northern Québec, Canada. *Global Ecol. Biogeogr.* 14, 307–313.

Baltzer, J.L., Nicola, D., Walker, X.J., Greene, D.F., Mack, M.C., submitted. Fire and the decline of fire-adapted black spruce in the boreal forest. *Science*.

Berkes, F., Davidson-Hunt, I.J., 2006. Biodiversity, traditional management systems, and cultural landscapes: examples from the boreal forest of Canada. *Int. Soc. Sci. J.* 58, 35–47.

Blaauw, M., 2010. Methods and code for 'classical' age-modelling of radiocarbon sequences. *Quat. Geochronol.* 5, 512–518.

Blaauw, M., Christen, J.A., 2011. Flexible paleoclimate age-depth models using an autoregressive gamma process. *Bayesian Anal.* 6, 457–474.

Blarquez, O., Vannière, B., Marlon, J.R., Daniau, A.-L., Power, M.J., Brewer, S., Bartlein, P.J., 2014. paleofire: an R package to analyse sedimentary charcoal records from the Global Charcoal Database to reconstruct past biomass burning. *Comput. Geosci.* 72, 255–261.

Boer, M.M., de Dios, V.R., Bradstock, R.A., 2020. Unprecedented burn area of Australian mega forest fires. *Nat. Clim. Change* 10, 171–172.

Boulanger, Y., Taylor, A.R., Price, D.T., Cyr, D., McGarrigle, E., Rammer, W., Sainte-Marie, G., Beaudoin, A., Guindon, L., Mansuy, N., 2017. Climate change impacts on forest landscapes along the Canadian southern boreal forest transition zone. *Landsc. Ecol.* 32, 1415–1431.

Braadbaart, F., Poole, I., 2008. Morphological, chemical and physical changes during charcoalification of wood and its relevance to archaeological contexts. *J. Archaeol. Sci.* 35, 2434–2445.

Brossier, B., Oris, F., Finsinger, W., Asselin, H., Bergeron, Y., Ali, A.A., 2014. Using tree-ring records to calibrate peak detection in fire reconstructions based on sedimentary charcoal records. *Holocene* 24, 635–645.

Campbell, I.D., McDonald, K., Flannigan, M.D., Kringayark, J., 1999. Long-distance transport of pollen into the Arctic. *Nature* 399, 29–30.

Cansler, C.A., McKenzie, D., 2014. Climate, fire size, and biophysical setting control fire severity and spatial pattern in the northern Cascade Range, USA. *Ecol. Appl.* 24, 1037–1056.

Chapin, F.S., McGuire, A.D., Ruess, R.W., Hollingsworth, T.N., Mack, M.C., Johnstone, J.F., Kasischke, E.S., Euskirchen, E.S., Jones, J.B., Jorgenson, M.T., 2010. Resilience of Alaska's boreal forest to climatic change. *Can. J. For. Res.* 40, 1360–1370.

Chaste, E., Girardin, M.P., Kaplan, J.O., Bergeron, Y., Hély, C., 2019. Increases in heat-induced tree mortality could drive reductions of biomass resources in Canada's managed boreal forest. *Landsc. Ecol.* 34, 403–426.

Conedera, M., Tinner, W., Neff, C., Meurer, M., Dickens, A.F., Krebs, P., 2009. Reconstructing past fire regimes: methods, applications, and relevance to fire management and conservation. *Quat. Sci. Rev.* 28, 555–576.

Coogan, S.C., Robinne, F.-N., Jain, P., Flannigan, M.D., 2019. Scientists' warning on wildfire—a Canadian perspective. *Can. J. For. Res.* 49, 1015–1023.

Crann, C.A., Patterson, R.T., Macumber, A.L., Galloway, J.M., Roe, H.M., Blaauw, M., Swindles, G.T., Falck, H., 2015. Sediment accumulation rates in subarctic lakes: insights into age-depth modeling from 22 dated lake records from the Northwest Territories, Canada. *Quat. Geochronol.* 27, 131–144.

Cwynar, L., Spear, R., 1995. Paleovegetation and paleoclimatic changes in the Yukon at 6 ka BP. *Géogr. Phys. Quaternaire* 49, 29–35.

Dalton, A.S., Margold, M., Stokes, C.R., Tarasov, L., Dyke, A.S., Adams, R.S., Allard, S., Arends, H.E., Atkinson, N., Attig, J.W., 2020. An updated radiocarbon-based ice margin chronology for the last deglaciation of the North American Ice Sheet Complex. *Quat. Sci. Rev.* 234, 106223.

De la Barrera, F., Barraza, F., Favier, P., Ruiz, V., Quense, J., 2018. Megafires in Chile 2017: monitoring multiscale environmental impacts of burned ecosystems. *Sci. Total Environ.* 637–638, 1526–1536. <https://doi.org/10.1016/j.scitotenv.2018.05.119>.

Djamali, M., Cilleros, K., 2020. Statistically significant minimum pollen count in Quaternary pollen analysis; the case of pollen-rich lake sediments. *Rev. Palaeobot. Palynol.* 275, 104156.

Dodd, W., Howard, C., Rose, C., Scott, C., Scott, P., Cunsolo, A., Orbinski, J., 2018. The summer of smoke: ecosocial and health impacts of a record wildfire season in the Northwest Territories, Canada. *Lancet Global Health* 6, S30.

Duffy, P.A., Walsh, J.E., Graham, J.M., Mann, D.H., Rupp, T.S., 2005. Impacts of large-scale atmospheric–ocean variability on Alaskan fire season severity. *Ecol. Appl.* 15, 1317–1330.

Dyke, A., 2005. Late Quaternary vegetation history of northern North America based on pollen, macrofossil, and faunal remains. *Géogr. Phys. Quaternaire* 59, 211–262.

Edwards, M.E., Bigelow, N.H., Finney, B.P., Eisner, W.R., 2000. Records of aquatic pollen and sediment properties as indicators of late-Quaternary Alaskan lake levels. *J. Paleolimnol.* 24, 55–68.

Environment Canada, 2017. Canadian Climate Normals 1971–2000.

Erni, S., Arseneault, D., Parisien, M.-A., Bégin, Y., 2017. Spatial and temporal dimensions of fire activity in the fire-prone eastern Canadian taiga. *Global Change Biol.* 23, 1152–1166.

Erni, S., Wang, X., Taylor, S., Boulanger, Y., Swystun, T., Flannigan, M., Parisien, M.-A., 2020. Developing a two-level fire regime zonation system for Canada. *Can. J. For. Res.* 50, 259–273.

Faegri, K., Iversen, J., 1989. *Textbook of Pollen Analysis*, fourth ed. John Wiley & Sons Ltd., Chichester.

Flannigan, M., Cantin, A.S., De Groot, W.J., Wotton, M., Newbery, A., Gowman, L.M., 2013. Global wildland fire season severity in the 21st century. *For. Ecol. Manag.*

- 294, 54–61.
- Flannigan, M.D., Wotton, B.M., Marshall, G.A., De Groot, W.J., Johnston, J., Jurko, N., Cantin, A.S., 2016. Fuel moisture sensitivity to temperature and precipitation: climate change implications. *Climatic Change* 134, 59–71.
- Fréchette, B., Richard, P.J., Grondin, P., Lavoie, M., Larouche, A.C., 2018. Histoire postglacière de la végétation et du climat des pessières et des sapinières de l'ouest du Québec, Mémoire de Recherche Forestière. Gouvernement du Québec, ministère des Forêts, de la Faune et des Parcs, Direction de la recherche forestière.
- Gaboriau, D.M., Asselin, H., Ali, A.A., Hély, C., Girardin, M.P., Under review. Main drivers of recent extreme wildfire years and identification of climatic thresholds on the territory of the Tłı̨chǫ First Nation, northwestern Canada. *Int. J. Wildland Fire*.
- Gajewski, K., Payette, S., Ritchie, J.C., 1993. Holocene vegetation history at the boreal forest–shrub-tundra transition in north-western Quebec. *J. Ecol.* 81, 433–443.
- Gajewski, K., Bunbury, J., Vetter, M., Kroeker, N., Khan, A.H., 2014. Paleoenvironmental studies in southwestern Yukon. *Arctic* 67, 58–70.
- Glew, J.R., 1991. Miniature gravity corer for recovering short sediment cores. *J. Paleolimnol.* 5, 285–287.
- Hansen, W.D., Fitzsimmons, R., Olnes, J., Williams, A.P., (in press). An alternate vegetation type proves resilient and persists for decades following forest conversion in the North American boreal biome. *J. Ecol.* <https://doi.org/10.1111/1365-2745.13446>.
- Hassol, S.J., 2005. Arctic Climate Impact Assessment - Scientific Report. Cambridge University Press.
- Hély, C., Chaste, E., Girardin, M.P., Remy, C., Blarquez, O., Bergeron, Y., Ali, A.A., 2020. A Holocene perspective of vegetation controls on seasonal boreal wildfire sizes using numerical paleoecology. *Front. Forests Global Chang.* 3, 106.
- Hennebelle, A., Aleman, J.C., Ali, A.A., Bergeron, Y., Carcaillet, C., Grondin, P., Landry, J., Blarquez, O., 2020. The reconstruction of burned area and fire severity using charcoal from boreal lake sediments. *Holocene* 30, 1400–1409.
- Higuera, P., 2009. CharAnalysis 0.9: Diagnostic and Analytical Tools for Sediment Charcoal Analysis. User's Guide. Montana State University, Bozeman, MT.
- Hoecker, T.J., Higuera, P.E., Kelly, R., Hu, F.S., 2020. Arctic and boreal paleofire records reveal drivers of fire activity and departures from Holocene variability. *Ecology*, e03096, 0.
- Images, Motic, 2018. Motic Images Plus 3.0 ML Software.
- IPCC, 2014. Climate Change 2014: Synthesis Report Summary for Policymakers. Contribution of Working Groups I, II and III to the Fifth Assessment Report of the Intergovernmental Panel on Climate Change.
- Jain, P., Wang, X., Flannigan, M.D., 2018. Trend analysis of fire season length and extreme fire weather in North America between 1979 and 2015. *Int. J. Wildland Fire* 26, 1009–1020.
- Juggins, S., 2017. Rjoia: Analysis of Quaternary Science Data. R Package Version, 0.9–21.
- Kasischke, E.S., Turetsky, M.R., 2006. Recent changes in the fire regime across the North American boreal region—spatial and temporal patterns of burning across Canada and Alaska. *Geophys. Res. Lett.* 33, L09703.
- Kaufman, D.S., Ager, T.A., Anderson, N.J., Anderson, P.M., Andrews, J.T., Bartlein, P.J., Brubaker, L.B., Coats, L.L., Cwynar, L.C., Duvall, M.L., 2004. Holocene thermal maximum in the western Arctic (0–180°W). *Quat. Sci. Rev.* 23, 529–560.
- Kelly, R., Chipman, M.L., Higuera, P.E., Stefanova, I., Brubaker, L.B., Hu, F.S., 2013. Recent burning of boreal forests exceeds fire regime limits of the past 10,000 years. *Proc. Natl. Acad. Sci. Unit. States Am.* 110, 13055–13060.
- Kochtubajda, B., Stewart, R.E., Flannigan, M.D., Bonsal, B.R., Cuell, C., Mooney, C.J., 2019. An assessment of surface and atmospheric conditions associated with the extreme 2014 wildfire season in Canada's Northwest Territories. *Atmos.–Ocean* 57, 73–90.
- Latifovic, R., Pouliot, D., Olthoff, I., 2017. Circa 2010 land cover of Canada: local optimization methodology and product development. *Rem. Sens.* 9, 1098.
- Lauriol, B., Lacelle, D., Labrecque, S., Duguay, C.R., Telka, A., 2009. Holocene evolution of lakes in the Bluefish basin, northern Yukon, Canada. *Arctic* 62, 212–224.
- Lecavalier, B.S., Fisher, D.A., Milne, G.A., Vinther, B.M., Tarasov, L., Huybrechts, P., Lacelle, D., Main, B., Zheng, J., Bourgeois, J., 2017. High Arctic Holocene temperature record from the Agassiz ice cap and Greenland ice sheet evolution. *Proc. Natl. Acad. Sci. Unit. States Am.* 114, 5952–5957.
- MacDonald, G., 1995. Vegetation of the continental Northwest Territories at 6 ka BP. *Géogr. Phys. Quaternaire* 49, 37–43.
- MacDonald, G.M., Edwards, T.W., Moser, K.A., Pienitz, R., Smol, J.P., 1993. Rapid response of treeline vegetation and lakes to past climate warming. *Nature* 361, 243–246.
- Macumber, A.L., Neville, L.A., Galloway, J.M., Patterson, R.T., Falck, H., Swindles, G., Crann, C., Clark, I., Gammon, P., Madsen, E., 2011. Paleoclimatological Assessment of the Northwest Territories and Implications for the Long-Term Viability of the Tibbitt to Contwoyto Winter Road, Part II: March 2010 Field Season Results. Open Report 2010–010. Northwest Territories. Geoscience office, NT.
- Mann, M.E., Rahmstorf, S., Kornhuber, K., Steinman, B.A., Miller, S.K., Coumou, D., 2017. Influence of anthropogenic climate change on planetary wave resonance and extreme weather events. *Sci. Rep.* 7.
- Meehl, G.A., Stocker, T.F., Collins, W.D., Friedlingstein, P., Gaye, T., Gregory, J.M., Kitoh, A., Knutti, R., Murphy, J.M., Noda, A., 2007. Global Climate Projections. In: Solomon, S., Qin, D., Manning, M., Chen, Z., Marquis, M., Averyt, K.B., Tignor, M., Miller, H.L. (Eds.), IPCC, 2007: Climate Change 2007: the physical science basis. contribution of Working Group I to the Fourth Assessment Report of the Intergovernmental Panel on Climate Change. Cambridge University Press, Cambridge, U.K., pp. 747–846.
- Mekonnen, Z.A., Riley, W.J., Randerson, J.T., Grant, R.F., Rogers, B.M., 2019. Expansion of high-latitude deciduous forests driven by interactions between climate warming and fire. *Nat. Plants* 5, 952–958.
- Mooney, S.D., Tinner, W., 2011. The analysis of charcoal in peat and organic sediments. *Mires Peat* 7, 1–18.
- Moser, K.A., MacDonald, G.M., 1990. Holocene vegetation change at treeline north of Yellowknife, Northwest Territories, Canada. *Quat. Res.* 34, 227–239.
- Mudelsee, M., 2013. Climate Time Series Analysis, Classical Statistical and Bootstrap Methods. Springer, Dordrecht.
- Mustaphi, C.J.C., Davis, E.L., Perreault, J.T., Pisaric, M.F., 2015. Spatial variability of recent macroscopic charcoal deposition in a small montane lake and implications for reconstruction of watershed-scale fire regimes. *J. Paleolimnol.* 54, 71–86.
- Nolan, R.H., Boer, M.M., Collins, L., Resco de Dios, V., Clarke, H., Jenkins, M., Kenny, B., Bradstock, R.A., 2020. Causes and consequences of eastern Australia's 2019–20 season of mega-fires. *Global Change Biol.* 26, 3756–3758. <https://doi.org/10.1111/gcb.14987>.
- NTENR, 2015. 2014 Fire season review report (No. 249–17(5)). Legislative assembly of the Northwest Territories. https://www.assembly.gov.nt.ca/sites/default/files/td_249-175.pdf.
- Olson, D.M., Dinerstein, E., Wikramanayake, E.D., Burgess, N.D., Powell, G.V., Underwood, E.C., D'amico, J.A., Itoua, I., Strand, H.E., Morrison, J.C., 2001. Terrestrial ecoregions of the world: a new map of life on Earth. *Bioscience* 51, 933–938.
- Oris, F., Ali, A.A., Asselin, H., Paradis, L., Bergeron, Y., Finsinger, W., 2014. Charcoal dispersion and deposition in boreal lakes from 3 years of monitoring: differences between local and regional fires. *Geophys. Res. Lett.* 41, 6743–6752.
- Parisien, M.-A., Barber, Q.E., Hirsch, K.G., Stockdale, C.A., Erni, S., Wang, X., Arseneault, D., Parks, S.A., 2020. Fire deficit increases wildfire risk for many communities in the Canadian boreal forest. *Nat. Commun.* 11, 2121.
- Pienitz, R., Smol, J.P., MacDonald, G.M., 1999. Paleolimnological reconstruction of Holocene climatic trends from two boreal treeline lakes, Northwest Territories, Canada. *Arctic Antarct. Alpine Res.* 31, 82–93.
- Polanco-Martinez, J.M., Medina-Elizalde, M.A., Goni, M.F.S., Mudelsee, M., 2019. BINCOR: an R package for estimating the correlation between two unevenly spaced time series. *R J.* 11, 170–184.
- Porter, T.J., Schoenemann, S.W., Davies, L.J., Steig, E.J., Bandara, S., Froese, D.G., 2019. Recent summer warming in northwestern Canada exceeds the Holocene thermal maximum. *Nat. Commun.* 10, 1631.
- Power, M.J., Marlon, J., Ortiz, N., Bartlein, P.J., Harrison, S.P., Mayle, F.E., Ballouche, A., Bradshaw, R.H., Carcaillet, C., Cordova, C., 2008. Changes in fire regimes since the Last Glacial Maximum: an assessment based on a global synthesis and analysis of charcoal data. *Clim. Dynam.* 30, 887–907.
- Price, D.T., Alfaro, R.I., Brown, K.J., Flannigan, M.D., Fleming, R.A., Hogg, E.H., Girardin, M.P., Lakusta, T., Johnston, M., McKenney, D.W., 2013. Anticipating the consequences of climate change for Canada's boreal forest ecosystems. *Environ. Rev.* 21, 322–365.
- Reimer, P.J., Bard, E., Bayliss, A., Beck, J.W., Blackwell, P.G., Ramsey, C.B., Buck, C.E., Cheng, H., Edwards, R.L., Friedrich, M., 2013. IntCal13 and Marine13 radiocarbon age calibration curves 0–50,000 years cal. BP. *Radiocarbon* 55, 1869–1887.
- Remy, C.C., Lavoie, M., Girardin, M.P., Hély, C., Bergeron, Y., Grondin, P., Oris, F., Asselin, H., Ali, A.A., 2017. Wildfire size alters long-term vegetation trajectories in boreal forests of eastern North America. *J. Biogeogr.* 44, 1268–1279.
- Richard, P., 1970. Atlas pollinique des arbres et de quelques arbustes indigènes du Québec. *Nat. Can.* 97 1–34 97-161; 241–306.
- Ritchie, J.C., 1985. Late-quaternary climatic and vegetational change in the lower Mackenzie basin, northwest Canada. *Ecology* 66, 612–621.
- Ritchie, J.C., Cwynar, L.C., Spear, R.W., 1983. Evidence from north-west Canada for an early Holocene Milankovitch thermal maximum. *Nature* 305, 126–128.
- SFOR, 2018. News and views: the burning hot summer of 2018. *Scand. J. For. Res.* 33, 724–727.
- Smith, A., Schismenos, S., Stevens, G., Hutton, L., Chalaris, M., Emmanouloudis, D., 2019. Understanding Large-Scale Fire Events: Megafires in Attica, Greece and California. United Nations Major Group for Children and Youth, USA, pp. 29–34. USA.
- Stephens, S.L., Burrows, N., Buyantuyev, A., Gray, R.W., Keane, R.E., Kubian, R., Liu, S., Seijo, F., Shu, L., Tolhurst, K.G., 2014. Temperate and boreal forest mega-fires: characteristics and challenges. *Front. Ecol. Environ.* 12, 115–122. <https://doi.org/10.1890/102332>.
- Sulphur, K.C., Goldsmith, S.A., Galloway, J.M., Macumber, A., Griffith, F., Swindles, G.T., Patterson, R.T., Falck, H., Clark, I.D., 2016. Holocene fire regimes and treeline migration rates in sub-arctic Canada. *Global Planet. Change* 145, 42–56.
- Swain, A.M., 1973. A history of fire and vegetation in Northeastern Minnesota as recorded in lake sediments. *Quat. Res.* 3, 383–390.
- Timoney, K.P., Mamet, S.D., Cheng, R., Lee, P., Robinson, A.L., Downing, D., Wein, R.W., 2019. Tree cover response to climate change in the forest-tundra of north-central Canada: fire-driven decline, not northward advance. *Ecoscience* 26, 133–148.
- Tinner, W., Hu, F.S., Beer, R., Kaltenrieder, P., Scheurer, B., Krähenbühl, U., 2006. Postglacial vegetational and fire history: pollen, plant macrofossil and charcoal records from two Alaskan lakes. *Veg. Hist. Archaeobotany* 15, 279–293.
- Trachsel, M., Telford, R.J., 2017. All age–depth models are wrong, but are getting

- better. *Holocene* 27, 860–869.
- Turco, M., von Hardenberg, J., AghaKouchak, A., Llasat, M.C., Provenza, A., Trigo, R.M., 2017. On the key role of droughts in the dynamics of summer fires in Mediterranean Europe. *Sci. Rep.* 7, 81.
- Upiter, L.M., Vermaire, J.C., Patterson, R.T., Crann, C.A., Galloway, J.M., Macumber, A.L., Neville, L.A., Swindles, G.T., Falck, H., Roe, H.M., 2014. Middle to late Holocene chironomid-inferred July temperatures for the Central Northwest Territories, Canada. *J. Paleolimnol.* 52, 11–26.
- Veraverbeke, S., Rogers, B.M., Goulden, M.L., Jandt, R.R., Miller, C.E., Wiggins, E.B., Randerson, J.T., 2017. Lightning as a major driver of recent large fire years in North American boreal forests. *Nat. Clim. Change* 7, 529–534.
- Viau, A.E., Gajewski, K., 2009. Reconstructing millennial-scale, regional paleoclimates of boreal Canada during the Holocene. *J. Clim.* 22, 316–330.
- Viau, A.E., Gajewski, K., Sawada, M.C., Fines, P., 2006. Millennial-scale temperature variations in north America during the Holocene. *J. Geophys. Res.: Atmosphere* 111, D09102.
- Vincent, J.-S., 1973. A palynological study for the little clay belt, northwestern Quebec. *Nat. Can.* 100, 59–70.
- Walker, X.J., Baltzer, J.L., Cumming, S.G., Day, N.J., Johnstone, J.F., Rogers, B.M., Solvik, K., Turetsky, M.R., Mack, M.C., 2018. Soil organic layer combustion in boreal black spruce and jack pine stands of the Northwest Territories, Canada. *Int. J. Wildland Fire* 27, 125–134.
- Wang, Y., Hogg, E.H., Price, D.T., Edwards, J., Williamson, T., 2014. Past and projected future changes in moisture conditions in the Canadian boreal forest. *For. Chron.* 90, 678–691.
- Wang, X., Parisien, M.-A., Taylor, S.W., Candau, J.-N., Stralberg, D., Marshall, G.A., Little, J.M., Flannigan, M.D., 2017. Projected changes in daily fire spread across Canada over the next century. *Environ. Res. Lett.* 12, 025005.
- Williams, J.W., 2006. *An Atlas of Pollen-Vegetation-Climate Relationships for the United States and Canada*. American Association of Stratigraphic Palynologists Foundation, Dallas, Texas.
- Winkler, M.G., 1985. Charcoal analysis for paleoenvironmental interpretation: a chemical assay. *Quat. Res.* 23, 313–326.
- Wotton, B.M., Flannigan, M.D., Marshall, G.A., 2017. Potential climate change impacts on fire intensity and key wildfire suppression thresholds in Canada. *Environ. Res. Lett.* 12, 095003.
- Zhang, X., Brown, R., Vincent, L., Skinner, W., Feng, Y., Mekis, E., 2011. Canadian Climate Trends, 1950–2007. In: *Canadian Biodiversity: Ecosystem Status and Trends 2010*, Technical Thematic Report No. 5. Canadian Councils of Resource Ministers, Ottawa, ON report.